

Modeling Uncertainty In Optical Communication Systems

Lawrence Fomundam

Department of Mathematics and Statistics

University of Maryland, Baltimore County

Undergraduate Honors Thesis for 2005

Advisor: John Zweck

Abstract

An experimental recirculating loop is traditionally used to study straight-line optical fiber communication systems. However, random polarization effects within a loop system are very different from those in a line because of the loop's periodicity. Experimentally, a device known as a polarization scrambler makes the loop model behave more like a straight line. The polarization scrambler accomplishes this by randomly rotating the polarization state of the light after each round trip of the loop. However, the distribution of these random rotations is biased. In this work, we use a biased model for the polarization scrambler to simulate the dependence of system performance on the biasing strength.

Table of Contents

Introduction	4 - 5
The Stokes Model for the Polarization State of Light	5 - 9
Overview of an Optical Fiber Communication System	9
Modeling an optical fiber communication system	9 - 10
Simulating the loop model	11 - 13
Computing total PDL within the simulation model	13 - 15
A real polarization scrambler	15 - 19
Modeling a real or biased polarization scrambler	19 - 20
Understanding the effects of a biased rotation model on signal propagation	21 - 24
Computer simulation of the entire system	24 - 26
Galtarossa's Formula	26
Results: PDFs and System Statistics.....	26 – 47
Static Case	27 - 38
Abrupt Case	38 - 47

Introduction

An optical fiber communication system is used to transmit data at very high speeds over long distances, for example from Baltimore to Paris. An optical signal is used to transmit the data using a sequence of light pulses. Since, binary data is transmitted, the power of each pulse determines whether a one or zero is transmitted.

In an optical fiber communication system, the fiber attenuates the signal being transmitted. Consequently, the power decreases as the signal propagates through the fiber over long distances. Amplifiers placed at regular intervals within the system periodically restore the power. The gain in the amplifiers compensates for loss in the preceding segment of fiber. In addition to restoring power, amplifiers add noise which causes errors. An error occurs when a transmitted one is received as a zero, or vice-versa. Nevertheless, optical fiber is a very good transmission medium and errors are extremely rare. An important research problem is to understand why errors occur and to measure the bit error ratio (BER) which is the probability that an error would occur.

In addition to noise, there are other effects called the polarization effects that can lead to errors. In particular, the signal can be further attenuated by an amount that depends on the polarization state of the light. This situation is called polarization dependent loss (PDL), because power loss depends on the polarization state. Amplifiers are the main source of PDL. The PDL in each amplifier is very small. However, as data propagates from transmitter to receiver it encounters many amplifiers and so the total PDL can be relatively large. The larger the total PDL the worse the bit error ratio can be.

Because an optical fiber communication system is difficult to study due to the rare occurrence of the errors and because the system ranges over long distances, researchers use a simple experimental model to facilitate the study of the system. This model is a recirculating loop that is between 100 and 500 km long. To experimentally emulate transmission over thousands of kilometers, the light travels around the loop many times before it is received.

A device called the polarization scrambler (PS) makes the loop behave more like a straight-line system. For each circulation of the loop, the polarization scrambler has a different random setting; i.e. it rotates light in a different manner. The probability density function (pdf) of these rotations is uniformly distributed for an ideal polarization scrambler. However, a real polarization scrambler does not have a uniformly distributed pdf. Its precise distribution function is not known. From our discussion so far, we know that the pdf of the total PDL in a loop system depends on the pdf of the rotations performed by the PS. A major goal of this work is to quantify the degree to which the pdf of total PDL depends on our model of a real PS.

The Stokes Model for the Polarization State of Light

Light can be described in terms of its polarization state. The light signal generated in the transmitter of an optical communication system is polarized. Polarized light is light whose electric field is a simple periodic function of position and time. Polarized light can be classified as linearly polarized, circularly polarized or elliptically polarized.

For linearly polarized light in an optical fiber, the magnitude and sign of the electric field vary with time t and distance z along the fiber, but the electric field vector is in a fixed direction transverse to the fiber (Hecht). Examples of linearly polarized light are horizontal and vertically polarized light. The electric field vector of horizontally polarized light is

$$\mathbf{E}_1(z,t) = \hat{\mathbf{i}} E_{ox} \cos(kz - \omega t) \quad (1a)$$

while that of vertically polarized light is

$$\mathbf{E}_2(z,t) = \hat{\mathbf{j}} E_{oy} \cos(kz - \omega t + \phi). \quad (1b)$$

Here $\hat{\mathbf{i}} = (1, 0, 0)$ and $\hat{\mathbf{j}} = (0, 1, 0)$ are unit vectors in the xy -plane, perpendicular to the propagation direction z along the fiber. The parameter k is the wave number and ω is the frequency of the light. The angle ϕ is a relative phase difference between \mathbf{E}_1 and \mathbf{E}_2 .

The parameters E_{ox} and E_{oy} are the amplitudes. In general, light that is linearly polarized oscillates in a plane whose normal is perpendicular to the direction of propagation.

The electric field of arbitrarily polarized light can be expressed in the form

$\mathbf{E}_3 = \mathbf{E}_1 + \mathbf{E}_2$, for some choice of the parameters E_{ox} , E_{oy} and ϕ . If $\phi = (2n + 1)\pi$,

where n is an integer, then

$$\mathbf{E}_3 = \mathbf{E}_1 + \mathbf{E}_2 = \left(\hat{\mathbf{i}} E_{ox} + \hat{\mathbf{j}} E_{oy} \right) \cos(kz - \omega t) \quad (1c)$$

is linearly polarized because the amplitude vector, given by $\hat{i} E_{ox} + \hat{j} E_{oy}$, has a fixed direction. If $\phi = -\pi/2 + 2n\pi$, where n is an integer and $E_{ox} = E_{oy} = E_o$ then

$$\mathbf{E}_3 = \mathbf{E}_1 + \mathbf{E}_2 = E_o \left(\hat{i} \cos(kz - \omega t) + \hat{j} \sin(kz - \omega t) \right). \quad (1d)$$

If the electric field is given by (1d) we say that the light is circularly polarized (Hecht).

Polarized light that is neither linearly nor circularly polarized is called elliptically polarized.

If we can successfully model the evolution of an optical signal as it propagates through optical fiber, then we might be able to predict the behavior of a real system. Stokes parameters provide a reduced model for describing an optical signal. They provide a natural and simple way of representing the polarization state of light. There are four Stokes parameters that are defined in terms of irradiances. Irradiance is the time-averaged value of the magnitude of the Poynting vector, which is proportional to the amplitude squared of the electric field. This time-average is taken over many pulses of light (Hecht).

Stokes parameters can be measured experimentally. In an experiment to measure the Stokes parameters, a beam of light is split into four identical beams. The first beam encounters an isotropic filter, the second encounters a horizontal polarizer, the third encounters a linear polarizer whose axis of transmission is 45° , and the fourth encounters a circular polarizer (Hecht) (see figure 1). The transmitted irradiances from each filter can be measured. Let us denote the transmitted irradiances through the first, second,

third and fourth filters by I_0, I_1, I_2 and I_3 respectively. The four Stokes parameters are then defined as

$$\begin{aligned} S_0 &= 2I_0 \\ S_1^* &= 2I_1 - 2I_0 \\ S_2^* &= 2I_2 - 2I_0 \\ S_3^* &= 2I_3 - 2I_0. \end{aligned}$$

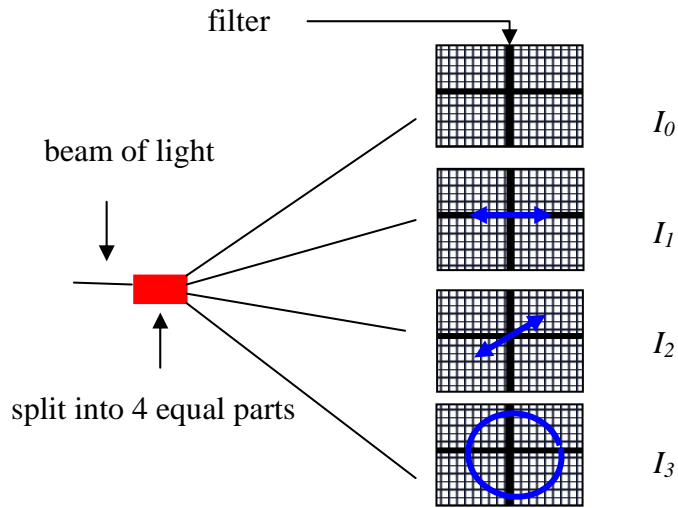


Figure 1
Experimental setup to measure Stokes parameters.

The Stokes parameter S_0 is the average power of a signal. By normalizing the average power, we can assume that S_0 has a maximum value of 1. The vector (S_1^*, S_2^*, S_3^*) is called the Stokes vector. The normalized Stokes vector is

$$(S_1, S_2, S_3) = \frac{S_1^* + S_2^* + S_3^*}{\sqrt{S_1^* + S_2^* + S_3^*}}. \quad (2)$$

Therefore, the polarization state (S_1, S_2, S_3) of an optical signal can be represented as a point on a unit sphere called the Poincare sphere. In the Stokes representation, vertically

polarized light, horizontally polarized light, and circularly polarized light are $(-1, 0, 0)$, $(1, 0, 0)$ and $(0, 0, \pm 1)$ respectively (Hecht).

Recall that polarized light is light whose electric field vector has a simple periodic dependence on position and time. The other extreme is unpolarized light. Its electric field vector undergoes a rapid succession of different random polarization states (Hecht). A natural light source is an example of unpolarized light. Partially polarized light is a mixture of polarized and unpolarized light. The degree of polarization (DOP) is defined

by
$$\text{DOP} = \frac{\sqrt{S_1^2 + S_2^2 + S_3^2}}{S_0}$$
. If $\text{DOP} = 1$ then the optical signal is polarized, while if

$\text{DOP} = 0$ then the signal is unpolarized. If $0 < \text{DOP} < 1$ then the signal is partially polarized.

Overview of an Optical Fiber Communication System

The basic components of an optical fiber communication system are a transmitter, optical fiber, optical amplifier and receiver. At the transmitter a modulator converts an electrical signal into an optical signal. The optical signal propagates through optical fiber to the receiver. Optical fiber is a wave-guide because it directs the optical signal along its cylindrical axis. As the signal propagates along the fiber's axis its polarization state undergoes random rotations on the Poincare sphere because of the fiber's structure.

Modeling an optical fiber communication system

An optical fiber communication system is a long-haul system covering thousands of kilometers. To study the statistical properties of straight-line optical links, we

immediately face the problem that it is not easy to access/and or reproduce sufficiently long links (Vinegoni). A natural and less expensive way to reproduce an optical fiber communication system is to design the recirculating loop model (Vinegoni). Researchers use a physical experimental model, which we illustrate in figure 2, to facilitate the study of a communication system. The loop is typically between 100 and 500km long.

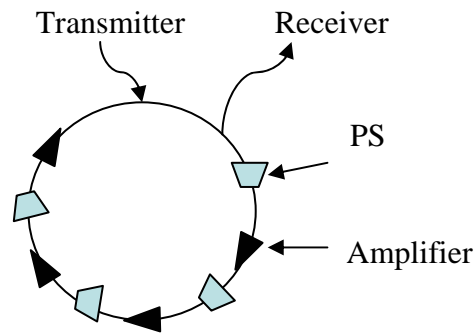


Figure 2

Physical model: The input signal is launched into the loop at the transmitter. After going through the recirculating loop N times the output is measured at the receiver.

The physical loop model attempts to capture the behavior of the straight-line system. After going around the loop once, identical fiber is encountered on subsequent round trips of the loop. This causes periodicity within the loop model that is not found in a straight-line system. The polarization scrambler is a physical component placed within a recirculating loop that is not present in a straight-line system. It is added in the model to reduce effects that are due to the periodicity of the loop (Sun). It does so by performing a different random rotation of light each round trip of the loop.

Simulating the loop model

A computer simulation of the loop model allows us to easily change the system parameters. We study the system by simulating the evolution of the Stokes parameters. Recall that Stokes parameters reduce the description of an optical signal to four numbers. In contrast to this reduced model, a full model describes an optical signal in terms of pulses which are a function of time, position, and polarization state.

For the results in my thesis, the propagation of light through optical fiber, polarization scramblers and optical amplifiers is described using linear models. The linear model of a system component is a four by four matrix that multiplies the input Stokes vector to that component. The result is an output Stokes vector that models the polarization state of light just after the component.

A three by three rotation matrix describes changes in the polarization state (S_1, S_2, S_3) due to the optical fiber. Any rotation matrix R_{rot} has the decomposition

$$R_{\text{rot}} = R_x(\psi)R_y(\theta)R_x(\phi).$$

The angles ψ , θ and ϕ are called Euler angles. This decomposition gives the rotation matrix R_{rot} an intuitive geometric interpretation. Consider what happens when the polarization state (S_1, S_2, S_3) is multiplied by R_{rot} . First, the vector (S_1, S_2, S_3) is rotated about the x -axis by an angle ϕ . Next, the resulting vector is rotated by an angle θ about the y -axis. Finally, the resulting vector is rotated by an angle ψ about the x -axis.

Because S_0 remains unchanged, our linear model for a signal propagating through optical fiber is

$$\mathbf{M}_{\text{PS}} = \begin{bmatrix} 1 & 0 & 0 & 0 \\ 0 & & & \\ 0 & \mathbf{R}_{\text{rot}} & & \\ 0 & & & \end{bmatrix}.$$

Recall that an optical fiber attenuates an optical signal propagating through it. Our rotation model has not accounted for this attenuation. In a real fiber we have polarization independent loss meaning that $S_0^{\text{out, fiber}} = e^{-\alpha L} S_0^{\text{in, fiber}}$ where L is the length of the fiber and α is the loss coefficient. When the signal goes through an amplifier the power is restored: $S_0^{\text{out, amplifier}} = G S_0^{\text{in, amplifier}}$. Since G is typically chosen so that $G = e^{\alpha L}$, in our model we ignore power loss in the fiber and gain in the amplifier.

Amplifiers add polarization dependent loss (PDL) which means that the power loss depends on the input Stokes parameters: $S_0^{\text{out}} = f(S_0^{\text{in}}, S_1^{\text{in}}, S_2^{\text{in}}, S_3^{\text{in}})$. Notice that the input Stokes vector to the amplifier is determined by the rotation of the Stokes vector in the previous fiber or polarization scrambler. We model PDL in the amplifier using the four by four matrix

$$\mathbf{M}_{\text{PDL}} = \begin{bmatrix} \frac{1+\alpha^2}{2} & \frac{1-\alpha^2}{2} & 0 & 0 \\ \frac{1-\alpha^2}{2} & \frac{1+\alpha^2}{2} & 0 & 0 \\ 0 & 0 & \alpha & 0 \\ 0 & 0 & 0 & \alpha \end{bmatrix}.$$

An optical signal that goes through an amplifier undergoes the linear transformation

$\mathbf{S}^{\text{out, amplifier}} = \mathbf{M}_{\text{PDL}} \mathbf{S}^{\text{in, amplifier}}$. The parameter, α , is the PDL per amplifier, which typically

has the value 0.1dB. For the PDL matrix \mathbf{M}_{PDL} there is a unique polarization state

(S_1, S_2, S_3) called the low-loss axis such that $\mathbf{M}_{\text{PDL}} \mathbf{S} = \mathbf{S}$ where $\mathbf{S} = (1, S_1, S_2, S_3)$. When

a signal's polarization state coincides with the low-loss axis it suffers the minimum possible power loss after going through the PDL element. Our PDL matrix has a low-loss axis of (1, 0, 0). The high-loss axis of a PDL element is the polarization state of the signal that undergoes the largest possible loss of power in the PDL element. In general the high-loss axis is antipodal to the low-loss axis on the Poincare sphere. For example, our PDL matrix has a high-loss axis of (-1, 0, 0).

Computing total PDL within the simulation model

In our simulation model we lump all the amplifiers in the loop and just consider a single amplifier with PDL matrix M_{PDL} . Similarly, we lump all the fiber segments and the polarization scrambler in the loop, and just consider a single rotation matrix $M_{\text{PS}}(i)$ for the i^{th} round trip of the loop (see figure 3). Theoretical work by Huttner *et al.* (Huttner) explains why the polarization scramblers and amplifiers can be lumped. The lumped model simplifies our computations. If the light, circulates the same loop N times, the system can be described using the transfer matrix

$$A = \prod_{i=1}^N M_{\text{PDL}} M_{\text{PS}}(i). \quad (3)$$

The four by four matrix, A , fully specifies the transfer function from input signal to

output signal; i.e.,
$$\begin{bmatrix} S_0^{\text{out}} \\ \mathbf{S}^{\text{out}} \end{bmatrix} = A \begin{bmatrix} S_0^{\text{in}} \\ \mathbf{S}^{\text{in}} \end{bmatrix}.$$

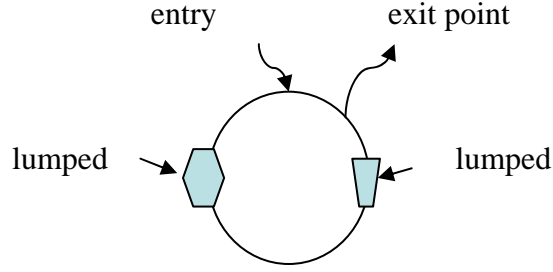


Figure 3

Simulation model: The input, which is \mathbf{S}^{in} , enters the system at the entry point. After going through the recirculating loop N times the output, \mathbf{S}^{out} , is measured at the exit point.

The total PDL, $\frac{S_0^{\text{out,max}}}{S_0^{\text{out,min}}}$, due to the system described by the matrix \mathbf{A} can be

computed from \mathbf{A} as follows. If we assume that the input Stokes vector has maximum power, $S_0 = 1$, then output power from the system is given by

$$S_0^{\text{out}} = A_{11} + \mathbf{A}_v^T \mathbf{S}_v \quad (4)$$

where $\mathbf{A}_v = (A_{12}, A_{13}, A_{14})$ and $\mathbf{S}_v = (S_1^{\text{in}}, S_2^{\text{in}}, S_3^{\text{in}})$. Because the power is maximized by varying over all input polarization states, if we choose $\mathbf{S}_v = \mathbf{A}_v$, then

$$S_0^{\text{out,max}} = S_0^{\text{out}} = A_{11} + \mathbf{A}_v^T \mathbf{A}_v = A_{11} + \|\mathbf{A}_v\|^2. \quad (5)$$

On the other hand, if we pick $\mathbf{S}_v = -\mathbf{A}_v$ then

$$S_0^{\text{out,min}} = S_0^{\text{out}} = A_{11} - \mathbf{A}_v^T \mathbf{A}_v = A_{11} - \|\mathbf{A}_v\|^2. \quad (6)$$

Therefore,

$$\text{total PDL} = \frac{S_0^{\text{out,max}}}{S_0^{\text{out,min}}} = \frac{A_{11} + \|\mathbf{A}_v\|^2}{A_{11} - \|\mathbf{A}_v\|^2}. \quad (7)$$

Notice that the total PDL is a random variable independent of the input polarization state.

The total PDL of the system is the maximum possible output power at the receiver divided by the minimum possible power optimized over all possible input polarization states at the transmitter. Large PDL is bad for the system. A large PDL indicates there is a polarization state for which the output power is very small. Small output power results in a low signal to noise ratio (SNR). Assuming, as is often the case, that the noise is unpolarized, the amount of noise is independent of the polarization state. Consequently, a low SNR means that there is a high probability for bit errors to occur.

A real polarization scrambler

We saw that a PS is an essential component in a loop system. To understand the behavior of a real PS we performed Monte Carlo experiments. From our Monte Carlo experiments we were able to describe the pdf of the rotations performed by a real PS and to show that these rotations are not uniformly distributed.

One of the simplest Monte Carlo experiments is a coin toss experiment. In this experiment we toss a coin M times, collect the results in a histogram and observe the frequency of obtaining a head or a tail in order to determine the coin's fairness. In this way, a Monte Carlo (MC) experiment approximates the distribution of a random variable. When data from a MC experiment is organized in a histogram, it approximates the probability density function of the random variable. As the number of samples, M , in the MC experiment increases the approximate pdf converges to the true pdf.

Similar to the coin toss experiment, my colleague Hai Xu performed three Monte Carlo experiments using the polarization scrambler which changes the input polarization state of an optical signal. In the first, second and third experiments the input polarization

states were the standard basis vectors $(1, 0, 0)$, $(0, 1, 0)$ and $(0, 0, 1)$ respectively. In the first experiment an input optical signal $\mathbf{S}^{\text{in, PS}} = (S_0, S_1, S_2, S_3) = (1, 1, 0, 0)$ is transmitted through a polarization scrambler element to obtain an output signal $\mathbf{S}^{\text{out, PS}} = \mathbf{M}_{\text{PS}}\mathbf{S}^{\text{in, PS}}$. Recall that the polarization scrambler has a negligible effect on the signal's power which is set to 1 by default. We repeat this procedure M times (each time \mathbf{M}_{PS} is chosen randomly), observe the output polarization on the Poincare sphere and map the results from the sphere to a histogram. The same experimental procedure is followed for the second and third experiments with input optical signals $\mathbf{S}^{\text{in, PS}} = (1, 0, 1, 0)$ and $\mathbf{S}^{\text{in, PS}} = (1, 0, 0, 1)$ respectively.

Xu's results are illustrated in figures 4a, 4b and 4c. The histograms contain $M = 6250$ samples which is large enough such that statistical error is not an issue. Notice that in the figures the number of samples varies from about 50 to 100 indicating that there is a bias within the polarization scrambler regardless of the input polarization state.

It was initially assumed that the polarization scrambler is ideal; that is it performs uniformly distributed rotations of the polarization state of a signal. However, the three Monte Carlo experiments in figure 4 show that the polarization scrambler is not ideal. In addition, the function by which the polarization scrambler rotates light is unknown. Therefore, in figure 4 we examined the distribution of rotations performed by the polarization scrambler. Since it is difficult to visualize a distribution of rotation matrices, we instead choose the three input polarization states and performed MC experiments to understand the distribution function for a real polarization scrambler.

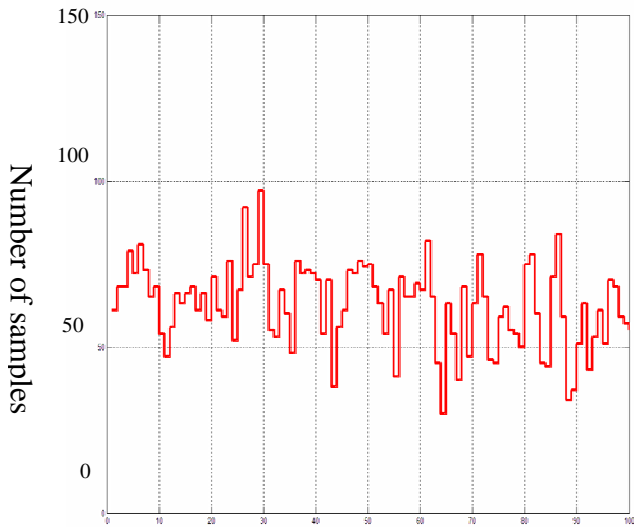


Figure 4a
 Distribution of output polarization states after going through a polarization scrambler with input polarization $(1, 0, 0)$.

150

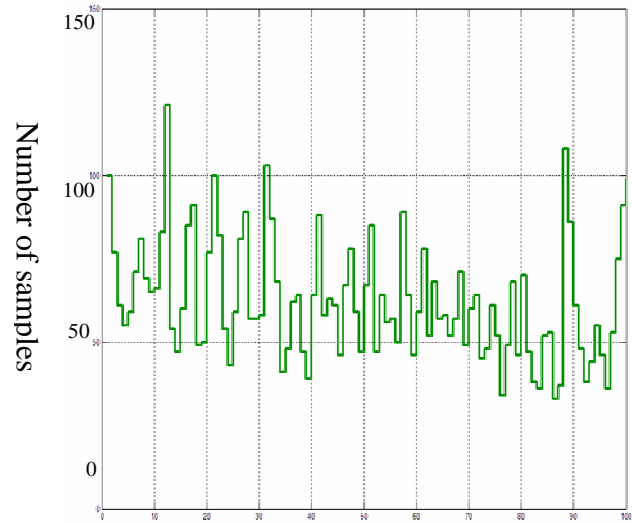


Figure 4a
 Distribution of output polarization states after going through a polarization scrambler with input polarization $(0, 1, 0)$.

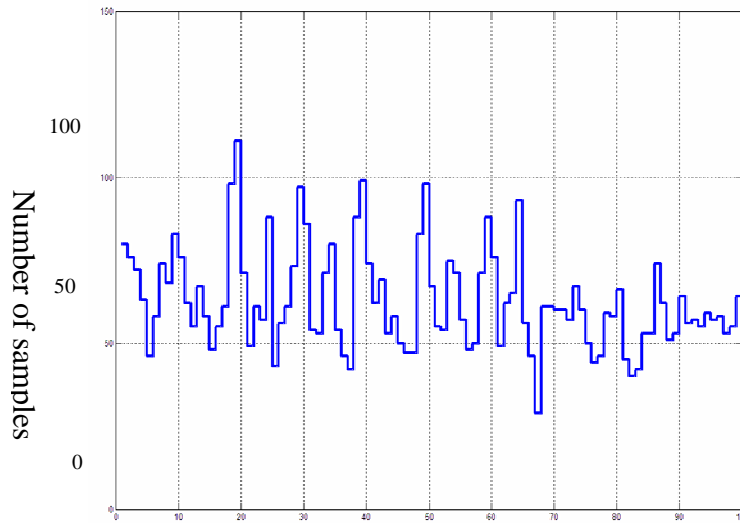


Figure 4c
 Distribution of output polarization states after going through a polarization scrambler with input polarization $(0, 0, 1)$.

In order to represent a distribution of polarization states (S_1, S_2, S_3) on a 1D histogram as in figures 4a, 4c and 4b we must define a mapping from the Poincare sphere to the 1D histogram. In spherical coordinates the Poincare sphere can be fully specified in terms of two angles Θ and Φ . Hence, the spherical coordinate representation offers a transformation from the sphere onto a rectangle in the plane. Consequently, a distribution of polarization states can be visualized using a two-dimensional histogram. We choose the spherical coordinate system so that $\Theta = \Theta_0$ is a circle of latitude and $\Phi = \Phi_0$ is a circle of longitude, where $0 \leq \Theta \leq \pi$ and $0 \leq \Phi \leq 2\pi$. We can use circles of latitude $(\Theta = \Theta_j \text{ for } j = 1 \text{ to } J)$ and longitude $(\Phi = \Phi_l \text{ for } l = 1 \text{ to } L)$ to define a grid on the sphere, and we can choose the grid curves so that the areas of the grid boxes are all the same. For each grid box B_{jl} let H_{jl} be the number of output polarization states that lie in this box.

We can visualize the two dimensional histogram H_{jl} as a one-dimensional histogram. The first J bins of the 1D histogram are obtained by going east around the J bins of the 2D histogram that are nearest to the North Pole. The next J bins are obtained by going south one bin from each of the first J bins, and so on until we reach the South Pole. Figure 6 illustrates these mappings from the Poincare sphere to a 2D histogram and from the 2D histogram to a 1D histogram.

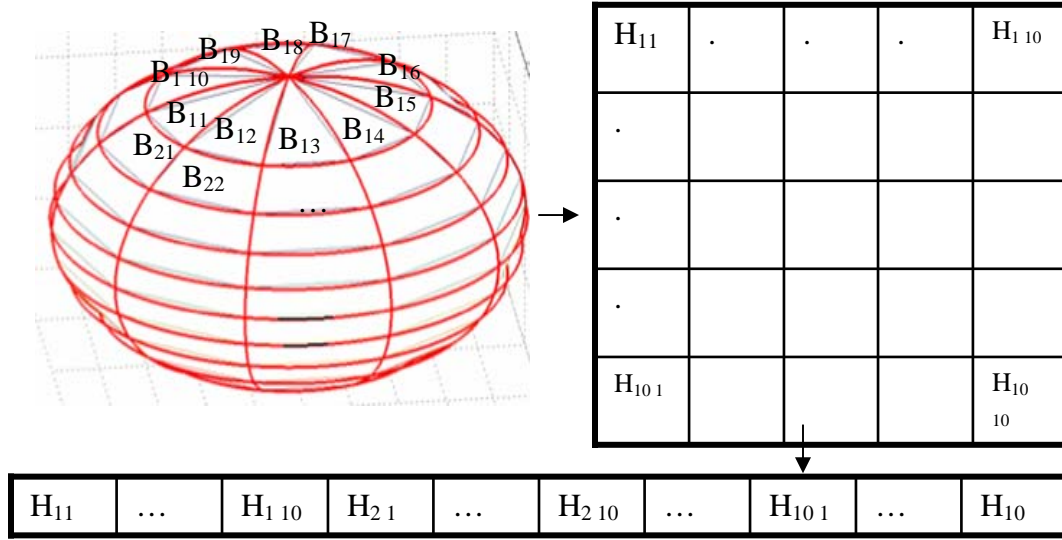


Figure 5

Illustrating the mapping from the Poincare sphere unto a 2D histogram and from the 2D histogram to a 1D histogram. The sphere partitioned into 100 equal area segments.

Modeling a real or biased polarization scrambler

In our simulations of a loop system we consider a reasonable rotation model for a biased (real) polarization scrambler. Recall that any rotation matrix R_{rot} has the decomposition $R_{rot} = R_x(\psi)R_y(\theta)R_x(\phi)$ where ψ , θ and ϕ are Euler angles. Therefore, to generate any rotation matrix we need to choose ψ , ϕ and θ appropriately.

To model an ideal PS we choose the Euler angles ψ , θ and ϕ from a uniform distribution with pdfs

$$f_\psi(x) = \frac{1}{2\pi} \quad \text{if } 0 \leq x \leq 2\pi \quad \text{else } 0,$$

$$f_{\phi}(x) = \frac{1}{2\pi} \quad \text{if } 0 \leq x \leq 2\pi \text{ else } 0,$$

$$f_{\cos\theta}(x) = \frac{1}{2} \quad \text{if } -1 \leq x \leq 1 \text{ else } 0.$$

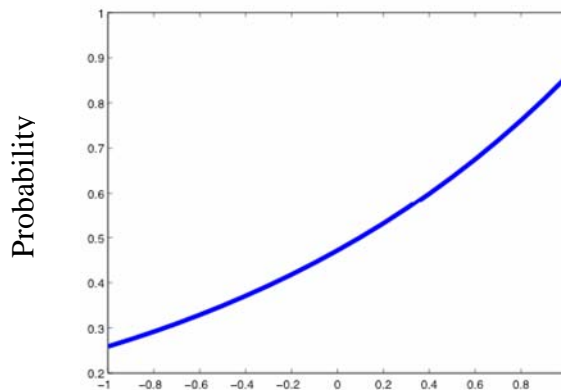
Because ψ , ϕ and $\cos\theta$ are uniformly distributed, R_{rot} is uniformly distributed in the space of three by three rotation matrices. For our biased PS model we choose ψ and ϕ from uniform distributions as above but now we choose θ from a biased distribution of $\cos\theta$ that is given by

$$f_{\beta}(\cos\theta) = \frac{\beta}{1 - e^{-2\beta}} e^{-\beta(1 - \cos\theta)} \quad \text{for } \beta > 0 \quad \text{if } |\cos\theta| \leq 1, \text{ else } 0.$$

$$f_{\beta}(\cos\theta) = \frac{1}{2} \quad \text{for } \beta = 0 \quad \text{if } |\cos\theta| \leq 1, \text{ else } 0.$$

Here, β is the biasing parameter. Note that as $\beta \rightarrow 0$, $f_{\beta}(\cos\theta) \rightarrow \frac{1}{2}$ for $|\cos\theta| \leq 1$.

Therefore, if $\beta = 0$ the biased model is equivalent to the unbiased model. As β increases, the pdf is more skewed to the right. In figure 4 we show the pdf of $\cos\theta$ with $\beta = 0.6$.

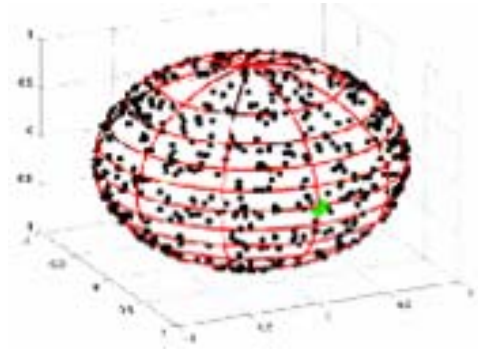


The pdf $f_{\beta}(\cos\theta)$ with $\beta = 0.6$.

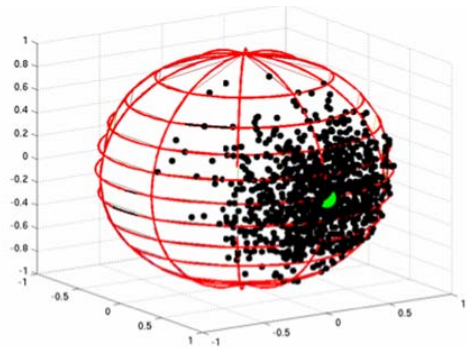
Understanding the effects of a biased rotation model on signal propagation

After performing Monte Carlo simulations (similar to those illustrated in figures 4a, 4b and 4c) using our biased PS model we obtained distributions of the output polarization states as shown in figures 7a, 7b and 7c. In figure 7a, we consider two cases both having an input polarization state, $(0, 0, 1)$, which we show as the large light dot. On the left, the rotations are uniformly distributed ($\beta = 0$), and we see that the output polarization states do indeed uniformly cover the Poincare sphere, as expected. On the right, the rotations are sampled from a biased pdf with biasing parameter $\beta = 10$. Notice that in this case the output polarization states are more heavily concentrated near $(0, 0, 1)$ than near $(0, 0, -1)$.

We use the definition of R_{rot} in terms of Euler angles to understand the distribution patterns in figures 7a, 7b and 7c. Let us consider the biased distribution in figure 7a. There is no change when $(1, 0, 0)$ is rotated about the x -axis by ϕ . If we rotate the resulting vector, $(1, 0, 0)$, about the y -axis by θ , it is on average close to $(1, 0, 0)$ since when β is large θ has a high probability of being near 0. Rotating the resulting vector about the x -axis by an angle ψ does not change its distance from $(1, 0, 0)$. Therefore, in figure 7a the points are more concentrated near $(1, 0, 0)$. Similar arguments can be used to understand figures 7b and 7c.



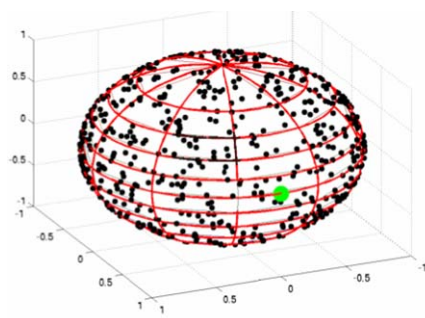
PS with



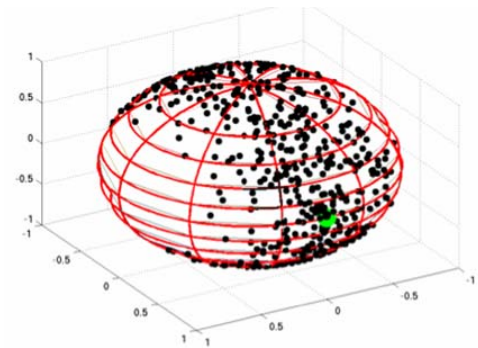
PS with $\beta = 10$

Figure 7a

Distribution of polarization states: For the distributions on the left and right, the input polarization state $(1, 0, 0)$ is the large light dot. After going through a PS the output polarization states, dark dots, are plotted on the Poincaré sphere. This is done for 1000 samples. For each sample the input polarization state is always $(1, 0, 0)$.



PS with $\beta = 0$



PS with $\beta = 10$

Figure 7b

Distribution of polarization states: For the distributions on the left and right, the input polarization state $(0, 1, 0)$ is the large light dot. After going through a PS the output polarization states, dark dots, are plotted on the Poincaré sphere. This is done for 1000 samples. For each sample the input polarization state is always $(0, 1, 0)$.

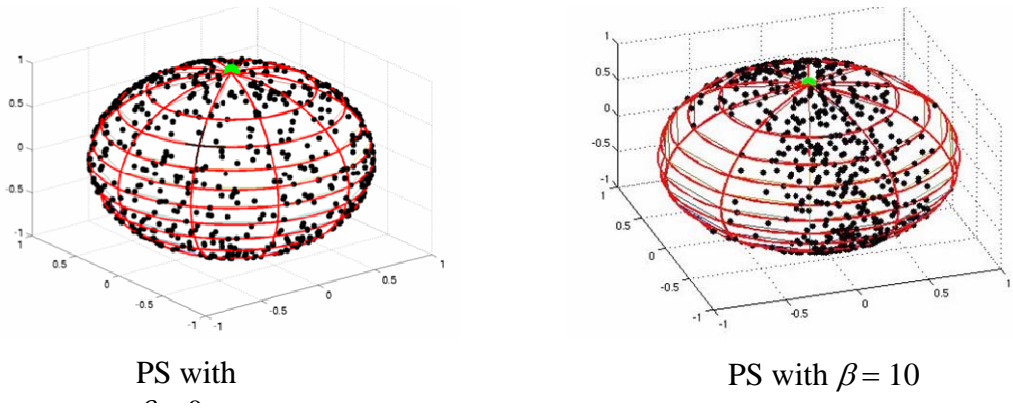


Figure 7c

Distribution of polarization states: For the distributions on the left and right, the input polarization state $(0, 0, 1)$ is the large light dot. After going through a PS the output polarization states, dark dots, are plotted on the Poincaré sphere. This is done for 1000 samples. For each sample the input polarization state is always $(0, 0, 1)$.

Xu's experimental data of a real polarization scrambler suggests that our biasing parameter should be a lot smaller than $\beta = 10$. Recall that in the experimental data (figure 4) samples generally vary between 50 to 100 elements which is by a factor of 2. For a biasing parameter $\beta = 0.6$ samples vary between 6000 to 16000 which is by a factor of 2.7 (see figure 8). Since this is comparable to a factor of 2 we deduce that $\beta = 0.6$ is a reasonable biasing parameter. Note that we are not attempting to match the shape of the histogram just the overall variability factor.

For a biasing parameter, $\beta = 0.6$, the biasing effects are very subtle on the sphere but more revealing on the histogram. By observing the front and back of the sphere in figure 8, we see that the points are more sparse on the back relative to the front. However, if we consider front and back separately, then both appear uniformly to be distributed.

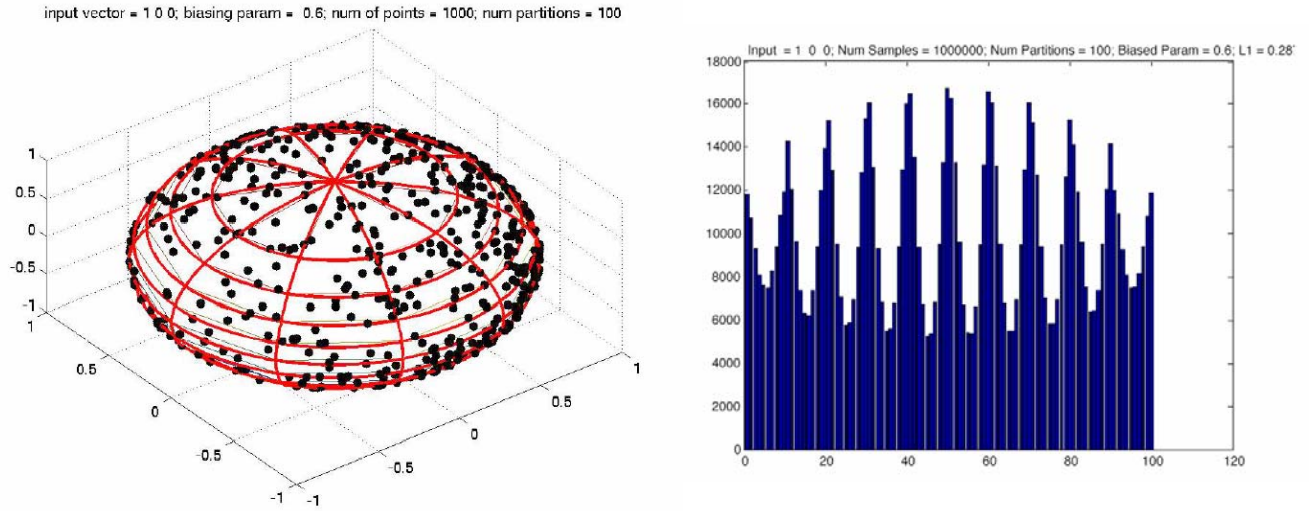


Figure 8

A distribution of output polarization states is seen on the left for a PS with $\beta=0.6$. On the right is its 1D representation.

Computer simulation of the entire system

We use MATLAB 7.0 to simulate our reduced model of an optical signal propagating through an optical fiber communication system. We simulate the system two different ways, which we refer to as the static case and the abrupt case. Recall that we used a lumped simulation model for simplicity. In addition, M_{PS} incorporates rotations done by both the fiber and the polarization scrambler.

The rotation matrix R_{rot} of real fiber changes over the course of time due to environmental factors such as temperature changes and mechanical vibrations. In fact

$R_{rot} = R_x(\psi)R_y(\theta)R_x(\phi)$ is

$$R_{rot} = \begin{pmatrix} \cos(\theta) & \sin(\theta)\cos(\psi) & -\sin(\theta)\sin(\psi) \\ -\sin(\theta)\cos(\phi) & \cos(\theta)\cos(\phi)\cos(\psi) - \sin(\phi)\sin(\psi) & -\cos(\theta)\cos(\phi)\sin(\psi) - \sin(\phi)\cos(\psi) \\ -\sin(\theta)\sin(\phi) & \cos(\theta)\sin(\phi)\cos(\psi) + \cos(\phi)\sin(\psi) & -\cos(\theta)\sin(\phi)\sin(\psi) + \cos(\phi)\cos(\psi) \end{pmatrix}$$

The time required for R_{rot} to change is longer than the time for light to propagate many times through the loop, i.e. it is longer than the time required to make a single measurement of the total PDL. We consider two different extremes for the time it takes for the rotation matrix of the fiber to change. At one extreme is the static case in which the fiber rotation R_{rot} does not change during the time that the M measurements of the total PDL are made. In this case, the transfer matrix $A^{(m)}$ for the m^{th} total PDL sample is

$$A^{(m)} = \prod_{i=1}^N M_{\text{PDL}} M_{\text{PS}}(m, i), \quad (8)$$

where $M_{\text{PS}}(m, i)$ is the four by four matrix that models the random rotation of the polarization scrambler in the i^{th} round trip of the loop for the m^{th} total PDL sample. A different random rotation matrix $M_{\text{PS}}(m, i)$ is chosen for each round trip and for each PDL sample. Here we are assuming that the fiber rotation $R_{\text{rot}} = I$, the identity matrix. At the other extreme is the abrupt case in which the fiber rotation changes randomly from one measurement of the total PDL to the next. In this case, the transfer matrix $A^{(m)}$ for the m^{th} total PDL sample is modeled by

$$A^{(m)} = \prod_{i=1}^N M_{\text{PDL}} M_{\text{FIBER}}(m) M_{\text{PS}}(m, i), \quad (9)$$

where $M_{\text{PS}}(m, i)$ is just as in the static case and $M_{\text{FIBER}}(m)$ is a 4x4 matrix that models the rotation due to the fiber in the loop for the m^{th} total PDL sample. In the abrupt case instead of changing the fiber rotation from sample to sample, we can instead think of the

fiber rotation as being fixed and regard the high and low loss PDL axes as changing randomly from one sample to the next.

Galtarossa's Formula

Galtarossa *et al.* derived an analytical formula for the pdf $f_x(x,t)$ of total PDL x for a static loop system with an unbiased polarization scrambler. The formula states that

$$f_x(x,t) = \frac{2x^2 e^{-x^2/2\gamma^2 t} \sinh(x/\gamma) e^{-t/2}}{\gamma^3 \sqrt{2\pi t}^3 x/\gamma}, \quad (11a)$$

where x is the total PDL and $\gamma = \frac{20}{\log_e 10}$. The variable t is a free parameter in their

theory that is related to the mean total PDL by

$$\langle x \rangle = \gamma \left[\sqrt{\frac{2t}{\pi}} e^{-t/2} + (1+t) \operatorname{erf} \left(\sqrt{\frac{t}{2}} \right) \right]. \quad (11b)$$

We determine a value for t by calculating an estimate of the mean total PDL $\langle x \rangle$ from a MC experiment and using a numerical root finding algorithm to solve for t in equation (11b). Although Galtarossa's formula was derived for a static loop system with an unbiased PS we also use it to find an analytical curve for a static loop system with a biased PS.

Results: PDFs and System Statistics

We want to determine the degree to which a biased PS affects the pdf of the total PDL and hence the pdf of the BER. In equation (7) we saw the dependence of total PDL

on the system transfer matrix. In equations (8), (9) and (10) we saw that total PDL also depends on the case under study (static case or abrupt case), the current sample m , the number of PDL elements N , and the biasing parameter β .

To understand the dependence of the total PDL on the parameters N and β we perform Monte Carlo experiments to obtain the pdf of total PDL in both the static and abrupt cases. Our experiments belong to two groups. For the first group we compute total PDL after traversing the loop 15 times (system has $N = 15$ PDL elements) while for the second group we traverse the loop 100 times (system has $N = 100$ PDL elements). In each group we chose 7 different values for the biasing parameter:

$\beta = 0, 0.1, 0.2, 0.3, 0.4, 0.5, 0.6$. For each Monte Carlo experiment within a group we choose $M = 1,000,000$ samples, and we set the PDL per amplifier to be $x_PDL = 0.1$ dB which corresponds to $\alpha = 0.9886$.

Static Case

Figure 9 shows the pdfs for the group containing 15 PDL elements while figure 10 shows the pdfs for the group containing 100 PDL elements. For each of the plots in either group the darker solid curve is the pdf for a loop system with a bias and the lighter solid curve is the pdf for a loop system with an unbiased PS. Both curves are obtain from MC experiments. The darker and lighter dashed curves are analytical fits for the biased and unbiased curves respectively. These curves are plotted on a semilog scale. The horizontal axis is total PDL measured in dB and the vertical axis, which is on the left, is probability density. An area under the pdf curves $\int_a^b f_x dx$ is the probability that $a \leq \text{total PDL} \leq b$. Notice that the tails of our Monte Carlo curves lack smoothness.

This is because large total PDL values have lower probabilities. Large total PDL values are very rare because they only occur when the rotations are such that the signal is repeatedly closely aligned with the low loss axes or the high loss axes. Consequently, there are very few samples that fall into the large total PDL bins, and so the statistical resolution is poor.

In figures 9, 10, 11, and 12, the thin solid curve at the bottom of the graph is the coefficient of variation curve shown using the linear scale on the right vertical axis. Recall that the pdfs computed from the MC experiments are approximations of the true pdfs. The coefficient of variation function tells us by how much the approximate pdf differs from the true pdf for a given total PDL value. In our pdfs (histograms) the number of hits in a bin is a random variable, which has a mean and a standard deviation. The probability density values we plot are estimates $\tilde{\mu}$ for the mean μ in each bin while $\tilde{\sigma}$ is the variance. By the central limit theorem μ approaches a gaussian distribution as $M \rightarrow \infty$. However, these values are not always accurate. To assess the accuracy of our pdfs at any point we would like to determine the probability that $\mu \in [\mu_0 - \sigma_0, \mu_0 + \sigma_0]$.

This is equivalent to the probability that $\frac{\mu}{\mu_0} \in \left[1 - \frac{\sigma_0}{\mu_0}, 1 + \frac{\sigma_0}{\mu_0}\right]$. If $\tilde{\sigma}$ is small $\frac{\tilde{\sigma}}{\mu_0}$ is also

small which implies that the probability that $\mu \in [\mu_0 - \sigma_0, \mu_0 + \sigma_0]$ is large since μ has a

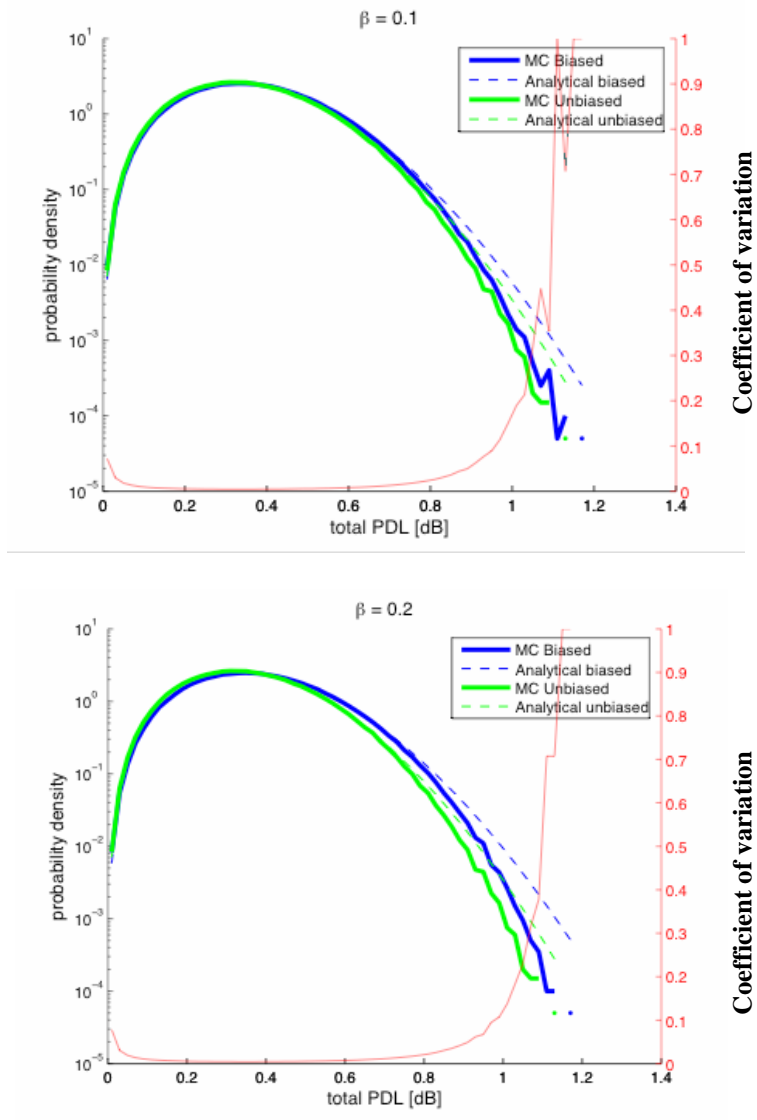
gaussian distribution. The coefficient of variation function is $g(x) = \frac{\sigma_0}{\mu_0} = \frac{\sqrt{1 - \mu_0}}{\sqrt{\mu_0} \sqrt{M - 1}}$.

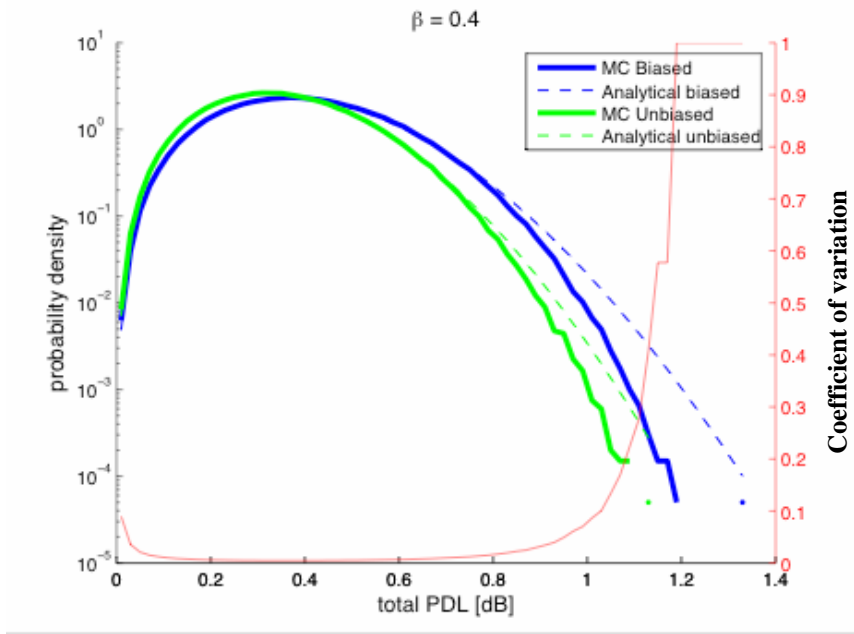
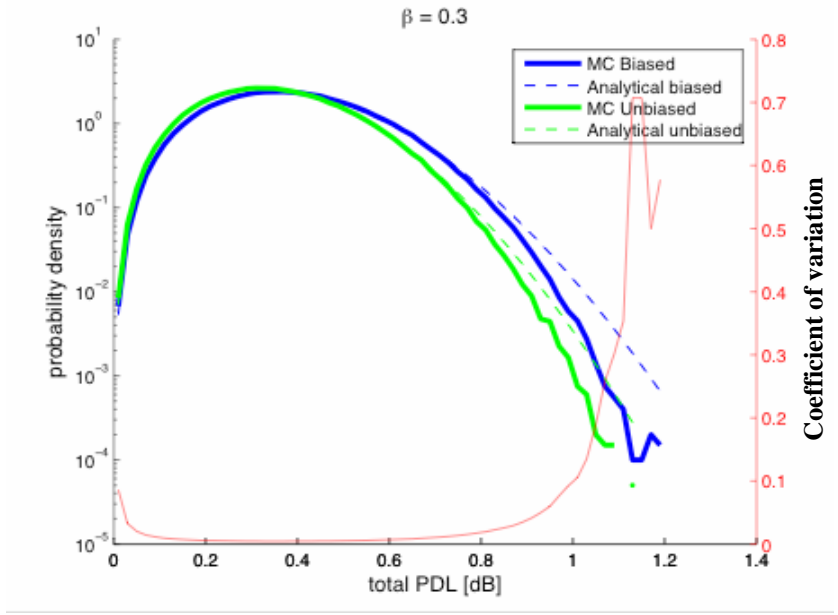
We computed the coefficient of variation function based on the fact that the number of hits in a bin is a binomial random variable. Here, x is the total PDL, M is the number of samples and $\tilde{\mu}$ is the fraction of hits within the bin containing x . If for some total PDL

value the coefficient of variation is zero, then at that total PDL value the approximate pdf and the true pdf are equal. As the coefficient of variation increases the approximate pdf deviates more and more from the true pdf as is the case in the tails. A small coefficient of variation means that the difference we see between the biased and unbiased pdf is real and not due to statistical error.

Figure 9

The probability density function of the total PDL in the static case. The number of PDL elements is $N = 15$. The biasing parameter increases from 0.1 to 0.6.





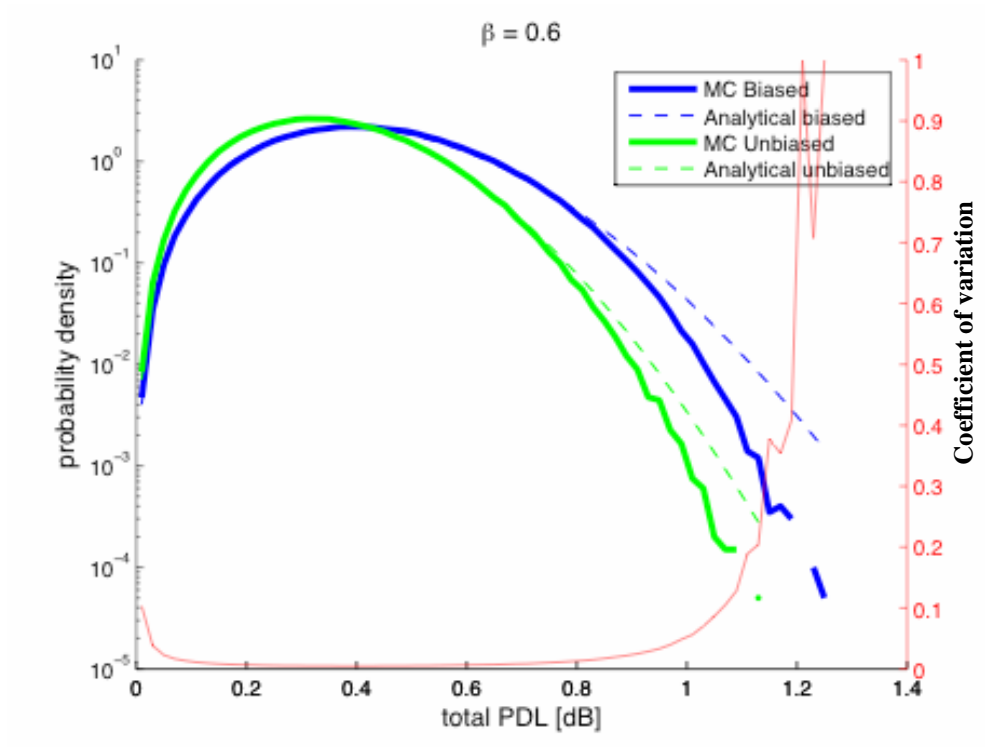
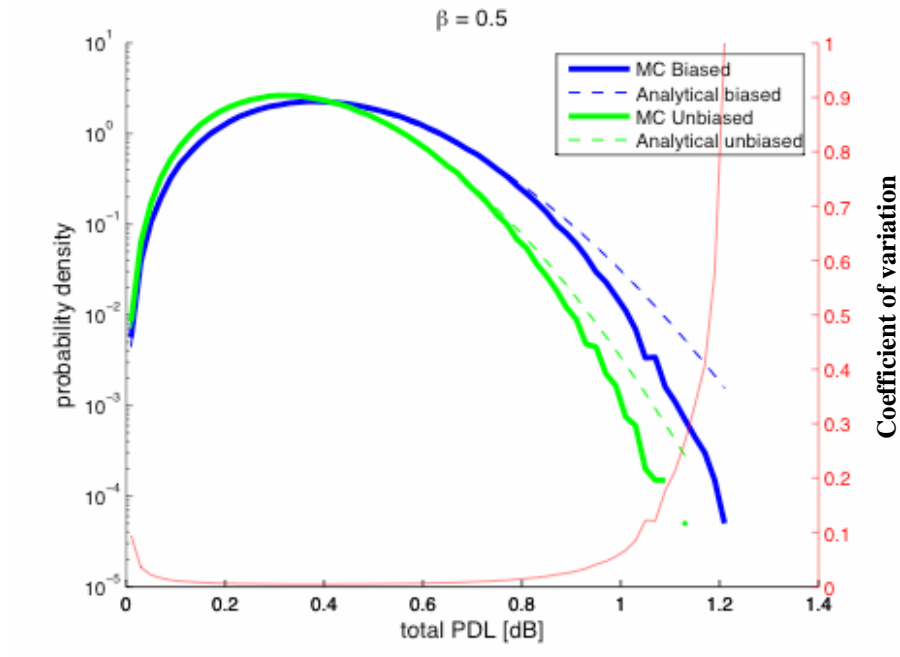
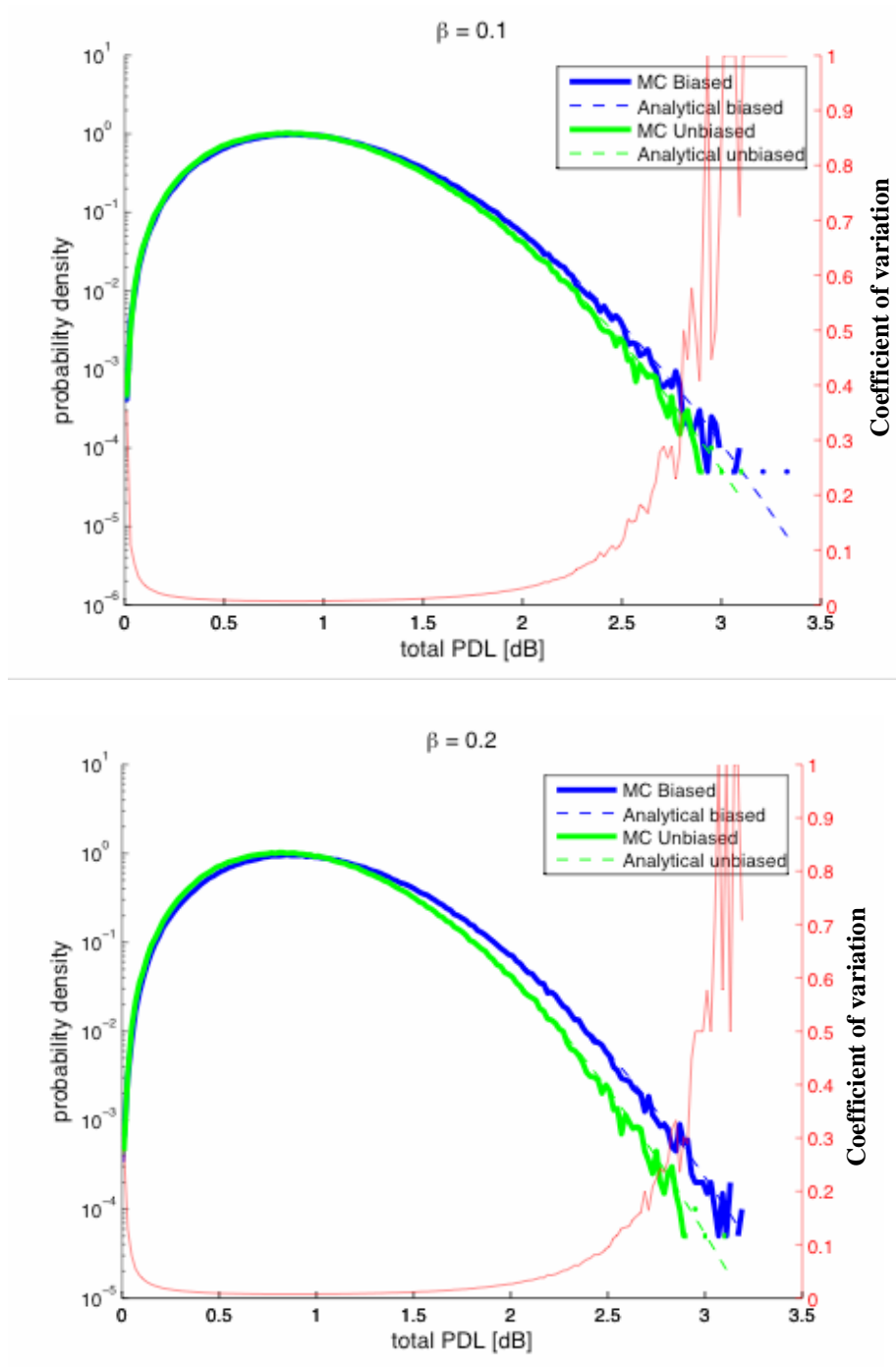
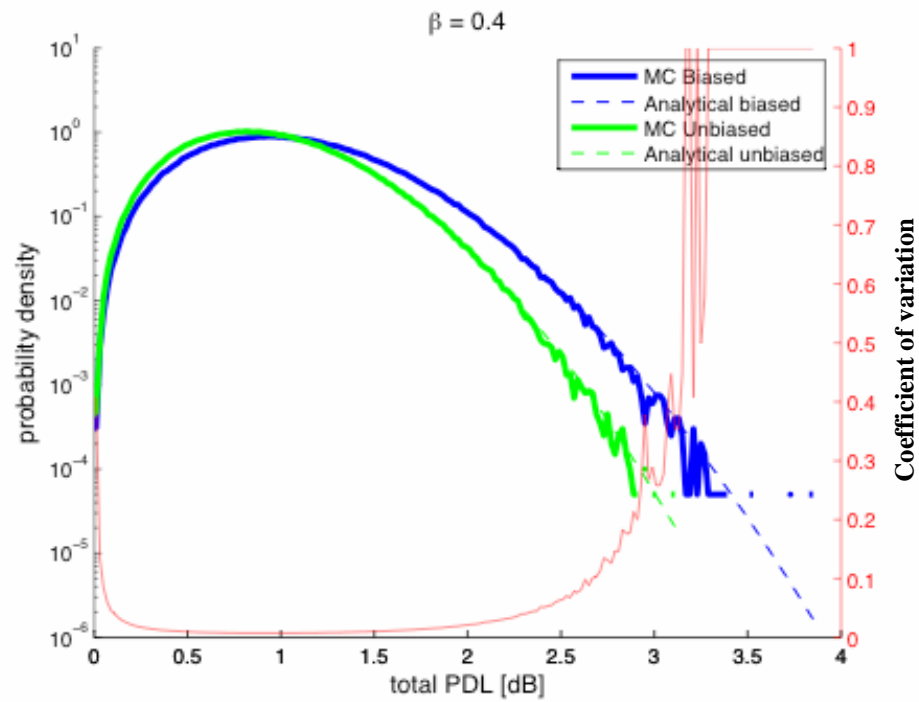
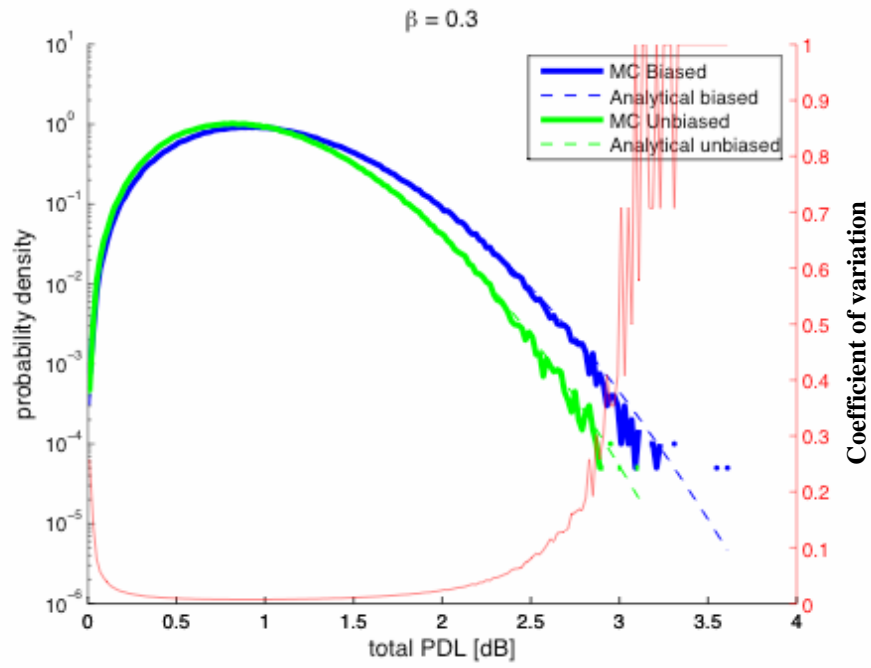
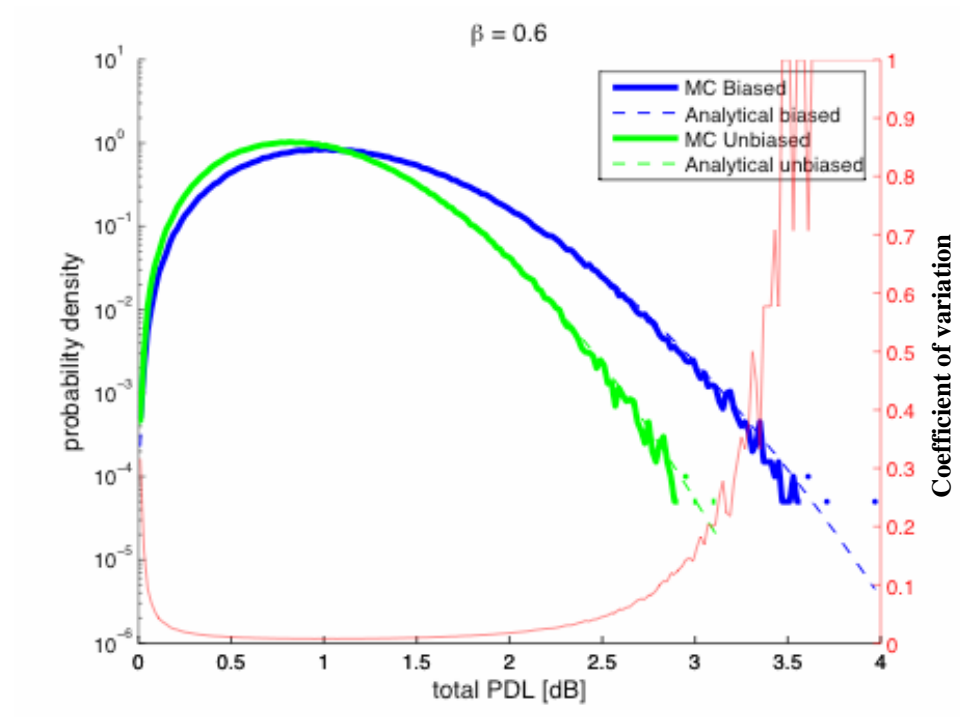
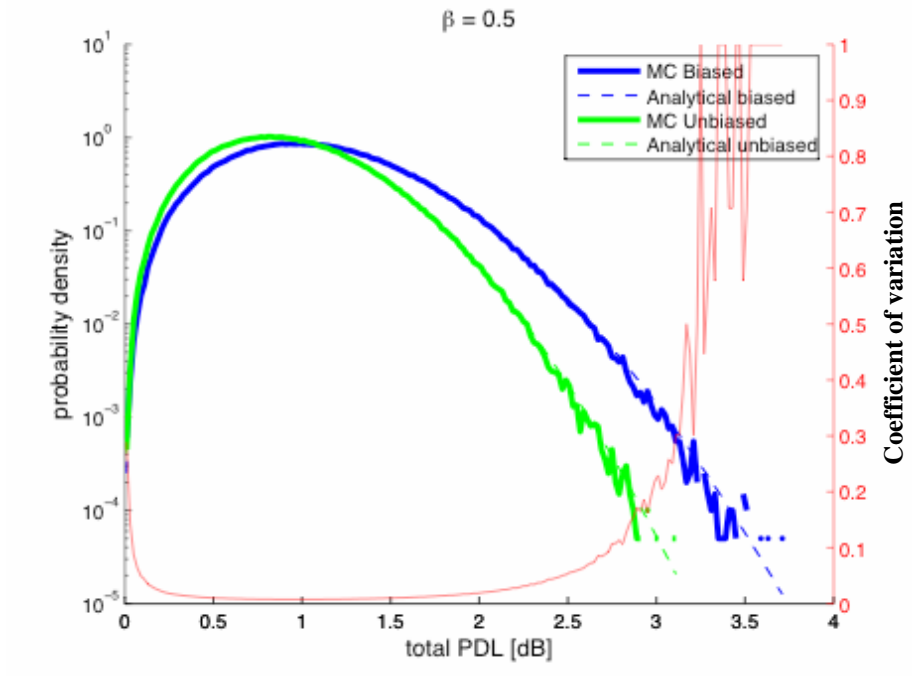


Figure 10

The pdf of the total PDL in the static case. The number of PDL elements is $N = 100$. The biasing parameter increases from 0.1 to 0.6.







Also notice that for 100 PDL elements the analytical curves agree very well with the curves from the Monte Carlo experiment. However, for 15 PDL elements they do not agree in the tails. This is because Galtarossa's formula works in the continuum limit, i.e. in the limit that the number of PDL elements approaches infinity, $N \rightarrow \infty$.

We saw in figure 7a that when the biasing parameter β is large and the input polarization state of the signal is close to the low-loss axis $(1, 0, 0)$ of the PDL, the output signal also tends to be close to the low loss axis. Similarly, if the input signal is close to the high loss axis $(-1, 0, 0)$ it will tend to stay close to the high loss axis when the biasing parameter is large. Therefore, in the biased static case as the loop is circulated many times, an input signal close to the low-loss axis will tend to remain near the low-loss axis and therefore tend to have a small total loss of power at the receiver, whereas an input signal that is close to the high loss axes will tend to remain near the high loss axis and therefore tend to have a large total loss of power at the receiver. Consequently, in the static case the total PDL will tend to be larger in the biased case than in the unbiased case, and the stronger the bias the larger the total PDL will tend to be. This explains why when the total PDL is large, the biased curve lies above the unbiased curve, i.e. why the probability of a large total PDL value is greater for the biased case than for the unbiased case.

The first and second columns in Tables 1 and 2 illustrate changes in the mean total PDL as a function of the biasing parameter for the static case. Table 1 shows the static case with 15 PDL elements while Table 2 shows the static case with 100 PDL elements. Notice that as the biasing parameter increases so does the mean of total PDL value. Also notice that a loop system with 15 PDL elements has a smaller mean than a

loop system with 100 PDL elements indicating that as the number of PDL elements increases the total PDL increases.

Table 1

Dependence of the mean and outage probability on the biasing parameter for 15 PDL elements for the static case

Biasing Parameter	Mean	0.8 dB Outage Probability
0	0.3579	0.0053
0.1000	0.3696	0.0076
0.2000	0.3818	0.0107
0.3000	0.3933	0.0145
0.4000	0.4062	0.0196
0.5000	0.4187	0.0256
0.6000	0.4316	0.0328

Table 2

Dependence of the mean and outage probability on the biasing parameter for 100 PDL elements for the static case

Biasing Parameter	Mean	2 dB Outage Probability
0	0.9225	0.0075
0.1000	0.9536	0.0107
0.2000	0.9852	0.0148
0.3000	1.0194	0.0203
0.4000	1.0527	0.0268
0.5000	1.0871	0.0348
0.6000	1.1233	0.0445

The first and third columns of Tables 1 and 2 show the dependence of the 0.8 dB and 2 dB outage probabilities on the biasing parameter. The 0.8 dB outage probability is the probability that total PDL exceeds 0.8 dB for a loop system containing 15 PDL elements. The 2 dB outage probability is the probability that total PDL exceeds 2 dB for a loop system containing 100 PDL elements. The outage probability can be used by system designers. A major goal in the design of optical fiber transmission systems is to minimize outage probability (Lima). A system designer may say for instance that the 2 dB outage probability of a system should not exceed 10^{-6} . This means that the probability that the total PDL is greater than 2 dB should be less than 10^{-6} . In Tables 1 and 2 notice that the outage probability increases with increasing biasing parameter. This is because with strong biasing the probability of getting larger total PDL values is greater. We have just observed changes in the pdf of total PDL as a function of the biasing parameter. However, the pdf with $\beta = 0.6$ is very important because it best reflects a real PS.

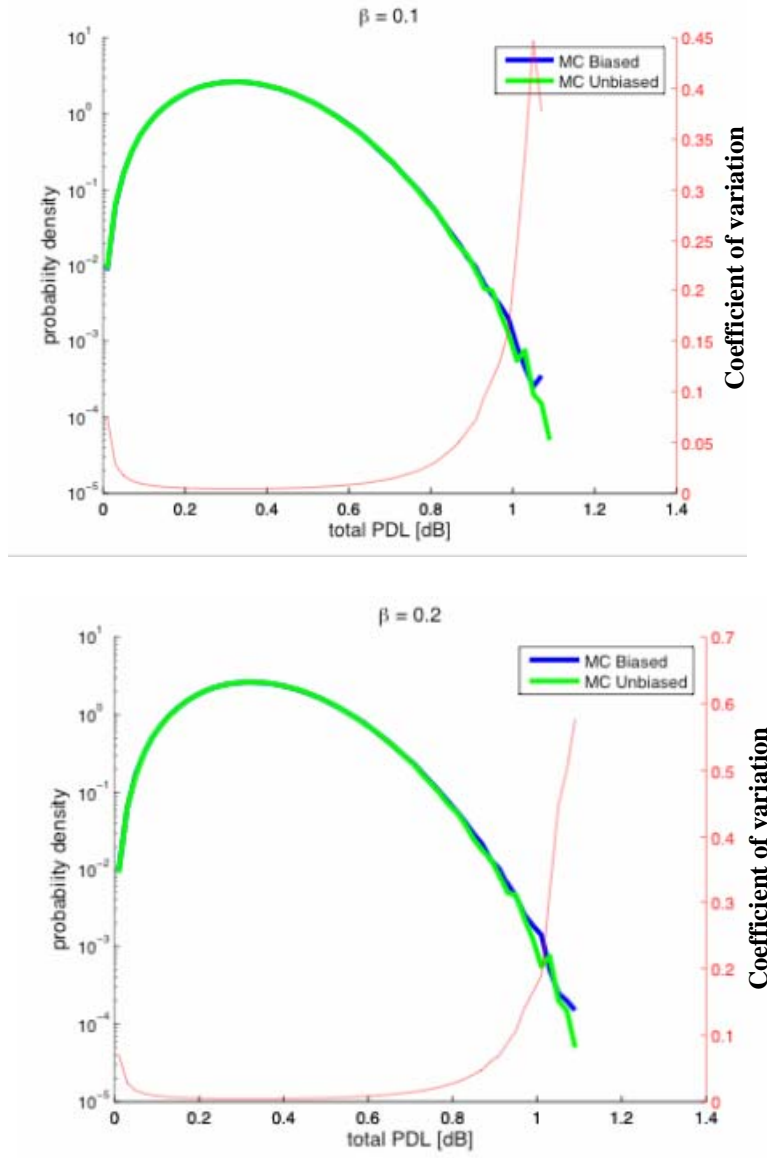
Abrupt case

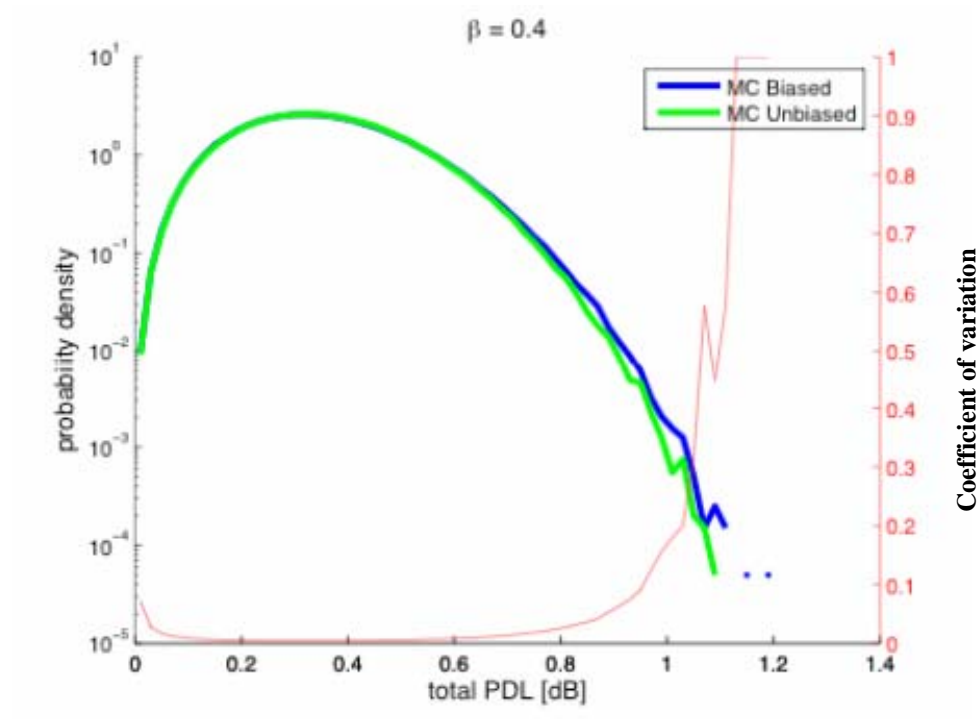
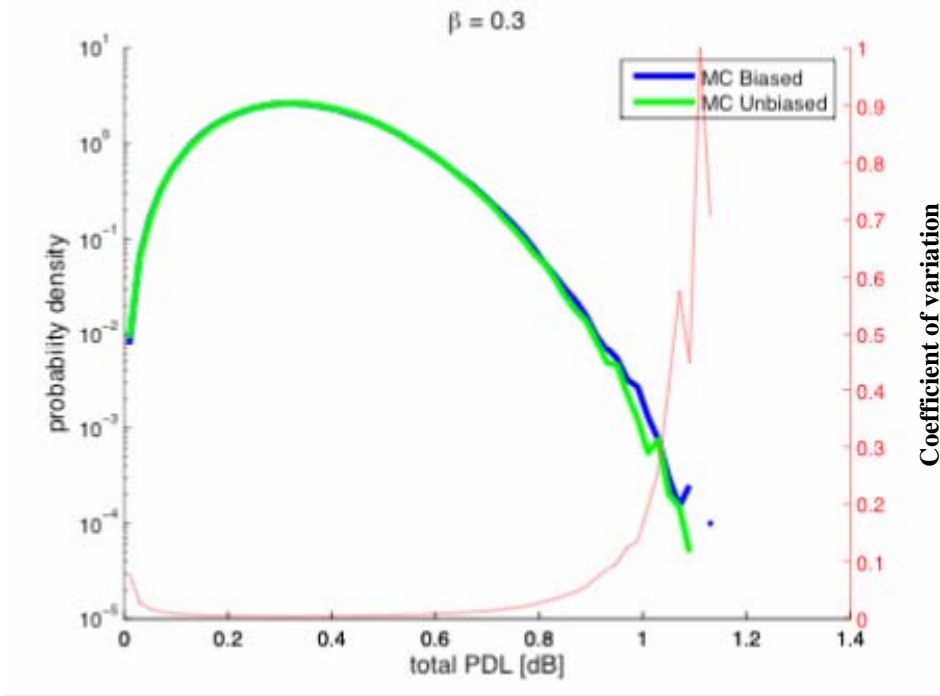
Figure 11 illustrates pdfs in the abrupt case for the group containing 15 PDL elements while figure 12 shows pdfs for the group containing 100 PDL elements. For each of the plots in either group the darker solid curve is the pdf for a loop system with a bias and the lighter solid curve is the pdf for a loop system with an unbiased PS. Both curves are obtained from MC experiments. These curves are plotted on a semi-log scale. The horizontal axis is total PDL measured in dB and the vertical axis, which is on the left, is probability. We have not shown analytical curves for the abrupt case because Galtarossa's formula is not a good analytical fit. In future work we will describe another

approach for obtaining an analytical fit.

Figure 11

The probability density function of the total PDL in the abrupt case. The number of PDL elements is $N = 15$. The biasing parameter increases from 0.1 to 0.6.





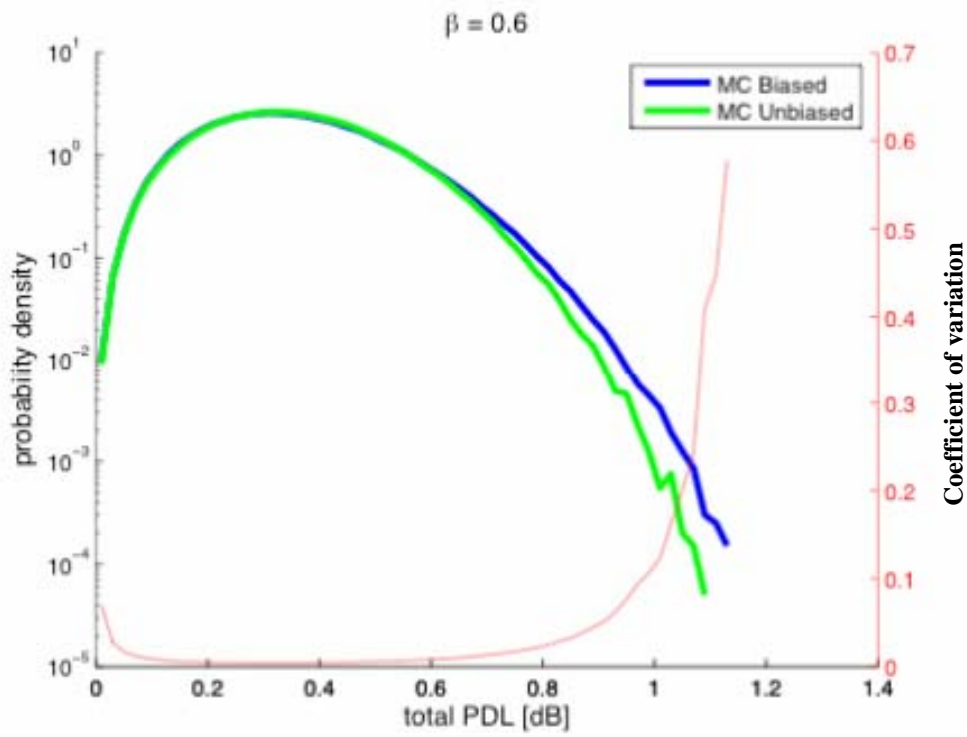
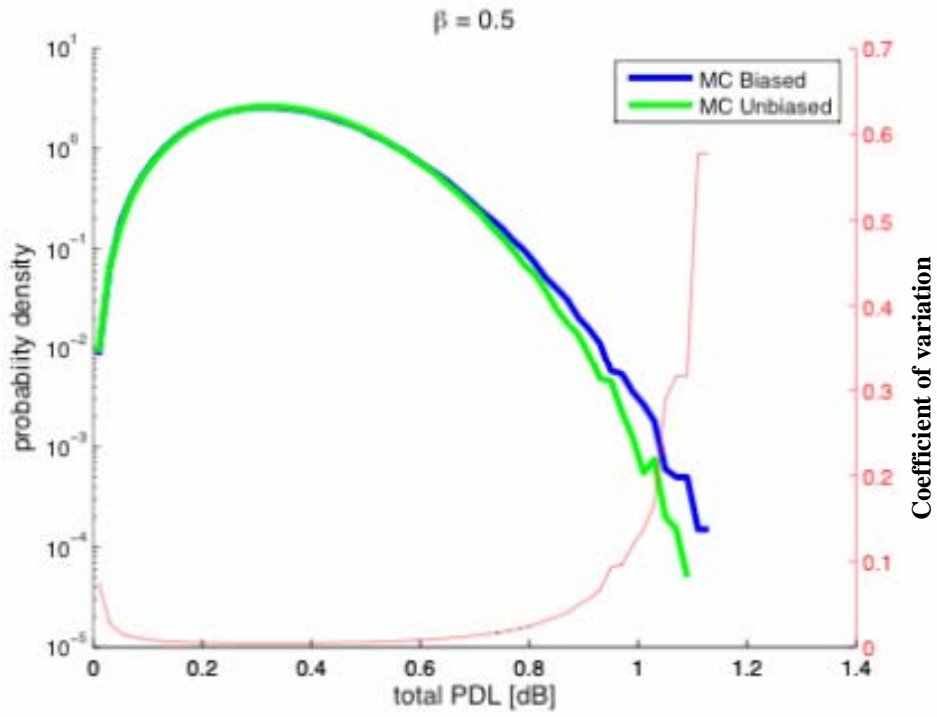
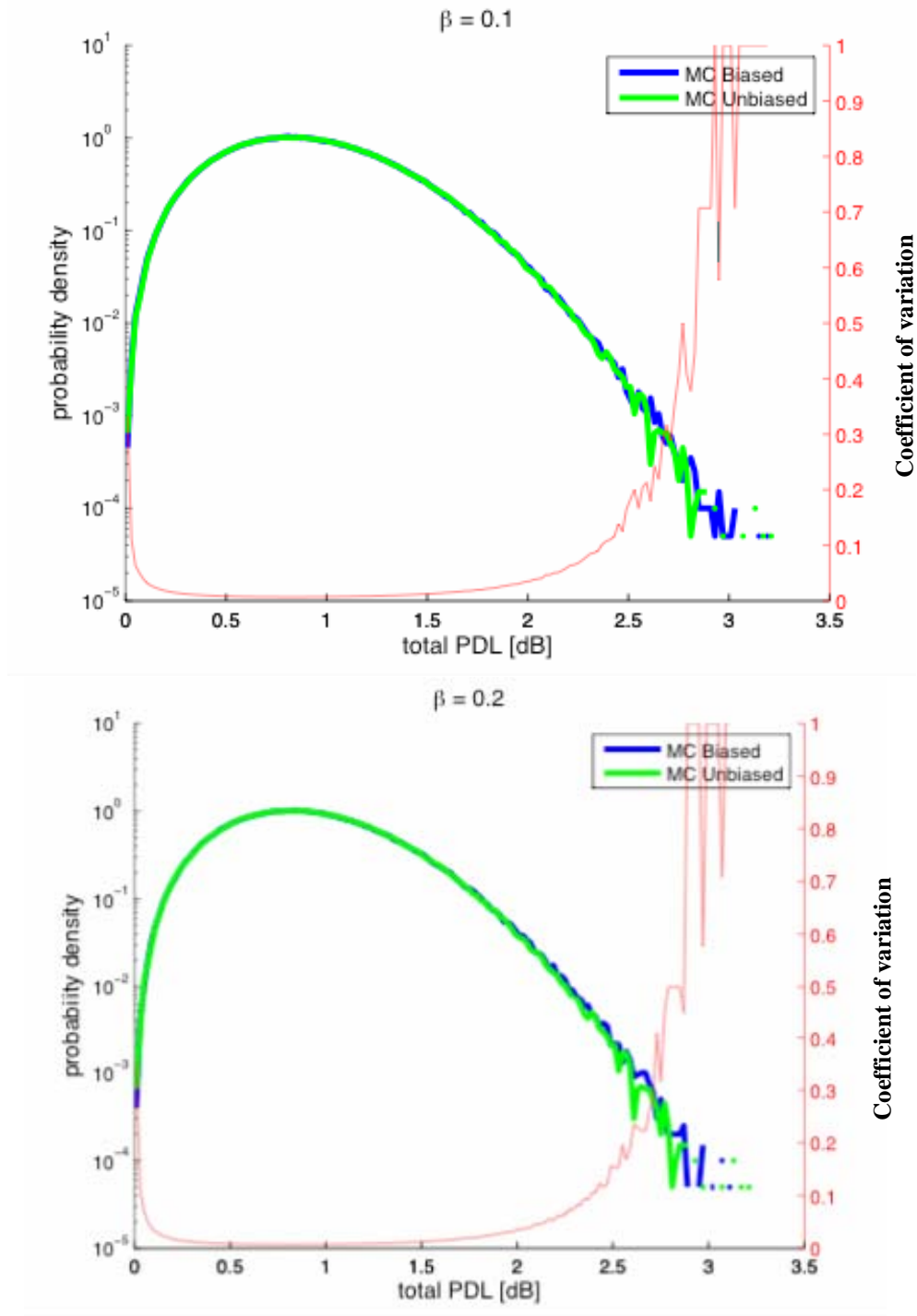
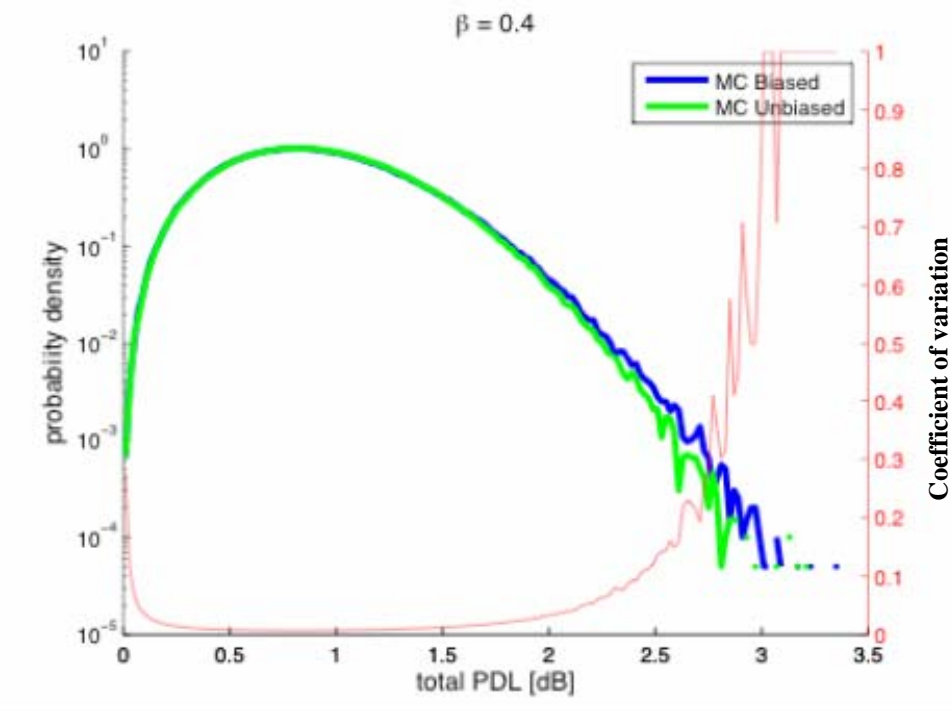
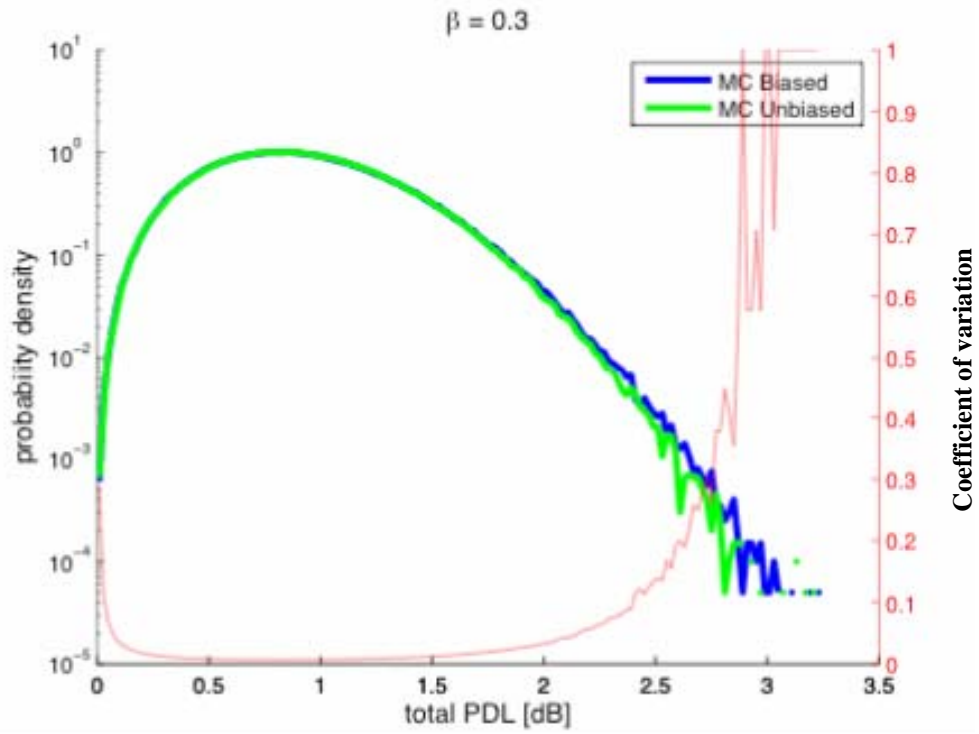
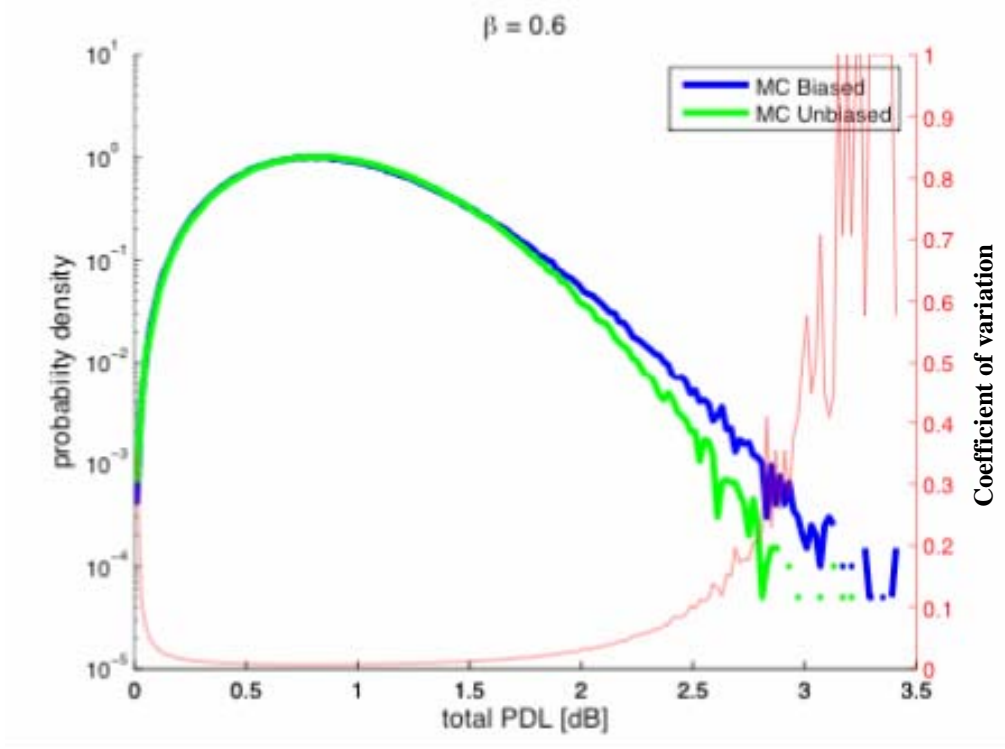
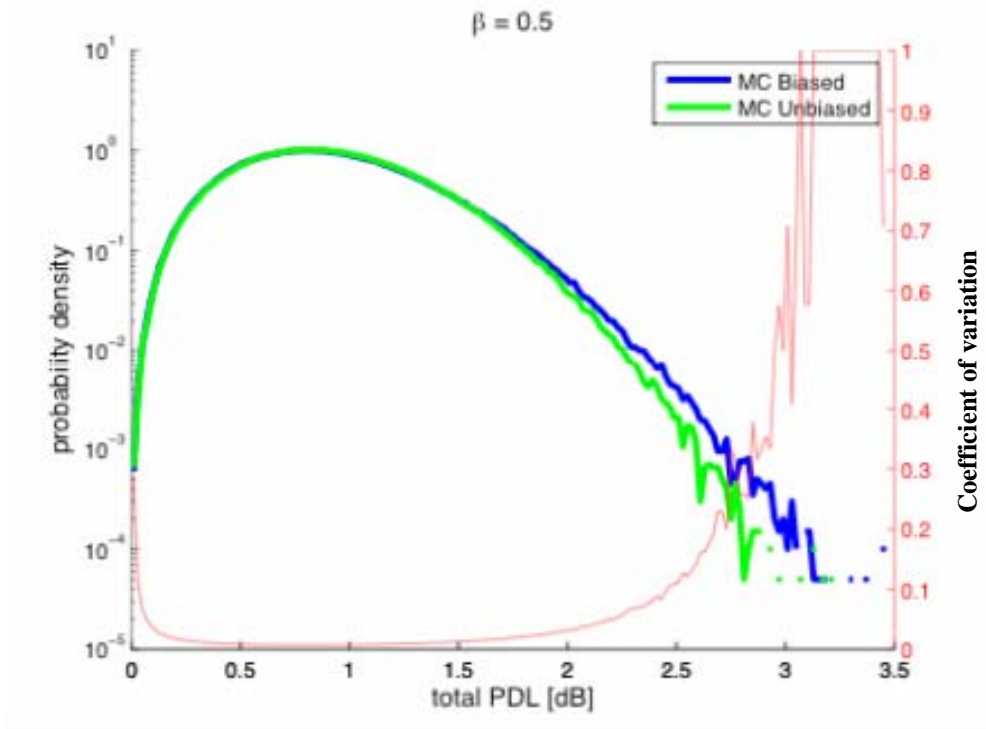


Figure 12

The probability density function of the total PDL in the abrupt case. The number of PDL elements is $N = 100$. The biasing parameter increases from 0.1 to 0.6.







The first and second columns in Tables 3 and 4 illustrate changes in the mean as a function of the biasing parameter for the abrupt case. Table 3 shows the abrupt case with 15 PDL elements while Table 4 shows the abrupt case with 100 PDL. Notice that for the abrupt case the mean and outage probability also increase as the biasing parameter increases.

Table 3

Dependence of the mean and outage probability on the biasing parameter for 15 PDL elements for the abrupt case

Biasing Parameter	Mean	0.8 dB Outage Probability
0	0.3582	0.0053
0.1000	0.3582	0.0053
0.2000	0.3583	0.0053
0.3000	0.3585	0.0054
0.4000	0.3592	0.0055
0.5000	0.3593	0.0055
0.6000	0.3602	0.0057

Table 4

Dependence of the mean and outage probability on the biasing parameter for 100 PDL elements for the abrupt case

Biasing Parameter	Mean	2 dB Outage Probability
0	0.9224	0.0075
0.1000	0.9225	0.0075
0.2000	0.9231	0.0075
0.3000	0.9240	0.0076
0.4000	0.9248	0.0077
0.5000	0.9265	0.0079
0.6000	0.9280	0.0080

The maximum possible total PDL value in either the abrupt or static case is given by $X_PDL * NUM_PDL$. Recall that $X_PDL = 0.1$ dB is the PDL per amplifier and NUM_PDL is the number of PDL elements in a fiber realization. Therefore, a fiber realization containing 15 PDL elements has a maximum total PDL = 1.5 dB while a fiber realization containing 100 PDL elements has a maximum total PDL = 10 dB. However, our pdfs in figure 10 (static case) have 100 PDL elements and a maximum total PDL value of 4 dB. Similarly, our pdfs in figure 12 (abrupt case) have 100 PDL elements and a maximum total PDL value of 3.5 dB. This is because the probability of getting a total PDL value greater than 3 dB is extremely small and we have not performed enough Monte Carlo simulations to obtain any samples with total PDL values in excess of 4 dB.

The main difference between the static and abrupt cases is that the low and high-loss axes change randomly in the abrupt case per fiber realization while they are fixed for all fiber realizations in the static case. But notice that in the abrupt case the mean values are smaller than those in the static case for a corresponding biasing parameter. The biasing matters much more in the static case. As the biasing parameter increases from 0.1 to 0.6, the 2 dB outage probability varies from 0.0075 to 0.0445 in the static case while it varies from 0.0075 to 0.0080 in the abrupt case. We expect the behavior of a PS in a real loop system to be intermediate between the static and abrupt cases and probably closer to the abrupt case.

Conclusions

In this work we suggested a model for a non-ideal polarization scrambler and used Monte Carlo experiments to determine the effect of our biased PS on the pdf of total PDL for a communication system. From experimental data we saw that a biased loop system with a biasing parameter of 0.6 is comparable to a real PS. By simulating different loop systems with different biasing strengths we also saw that total PDL increases with increasing biasing strength and the mean PDL is greater in the static case. Recall that the biasing function of a real PS is unknown. A question that remains unanswered is how an arbitrary bias in the PS affects the system pdf. Recall that the ultimate goal of simulating a straight-line system is to specify system parameters for the design of an actual communications system. My thesis is step toward this goal because it examines pdfs that describe the overall behavior of the system.

References

- A. Galtarossa and L. Palmieri. "The Exact Statistics of Polarization-Dependent Loss in Fiber-Optics Links," *IEEE Photon. Technol. Lett.*, vol. 15, pp. 45 – 47, Jan. 2003.
- E. Hecht. "Optics," Third Edition, Addison-Wesley, MA.
- B. Huttner, C. Geiser, and N. Gisin, "Polarization-Induced Distortions in Optical Fiber Networks with Polarization-Mode Dispersion and Polarization-Dependent Losses," *IEEE J. Select. Topics Quantum Electron.*, vol. 6, pp. 317- 329, Mar./Apr. 2000.
- I. T. Lima Jr., A. O. Lima, J. Zweck and C. R. Menyuk. "Efficient Computation of Outage Probabilities Due to Polarization Effects in a WDM System Using a Reduced Stokes Model and Importance Sampling," *IEEE Photon. Technol. Lett.*, vol. 15, pp. 45 – 47, Jan. 2003.
- A. Papoulis and S. U. Pillai. "Probability, Random Variables and Stochastic Processes," Fourth Edition, McGraw-Hill, Boston, MA.
- Y. Sun, A.O. Lima, I. T. Lima Jr., J. Zweck, L. Yan, C. R. Menyuk, and G. M. Carter. "Statistics of the System Performance in a Scrambled Recirculating Loop With PDL and PDG," *IEEE Photon. Technol. Lett.*, vol. 15, pp. 1067 – 1069, Aug. 2003.
- C. Vinegoni, M. Karlsson, M. Petersson, and H. Sunnerud. "The Statistics of Polarization-Dependent Loss in a Recirculating Loop," *J. Lightwave Technol.*, vol. 22, pp. 1593 – 1600. Apr. 2003.
- D. Wang and C. R. Menyuk. "Calculation of Penalties Due to Polarization Effects in Long-Haul WDM System Using a Stokes Parameter Model," *J. Lightwave Technol.*, vol. 19, pp. 487 – 494. Apr. 2001.
- Q. Yu, L.S. Yan, S. Lee, Y. Xie, and A. E. Willner. "Loop-Synchronous Polarization Scrambling Technique for Simulating Polarization Effects Using Recirculating Fiber Loops," *J. Lightwave Technol.*, vol. 21, pp. 1593 – 1600. Jul. 2003.